constants, a yield $f_{CH_3O} = 0.15 \pm 0.08$ is obtained.

F + Methanol. The products of this reaction have been studied by several groups (see Table III). The technique of Hoyermann et al.[8] is the most similar to ours; however, they found the HF and DF mass spectrometer signals to exhibit a memory effect and their branching fractions for methoxy formation have large uncertainties. This effect was not observed in the present study; however, some background signals were surprisingly large. In the F + CH_3OD reaction, for instance, the background at m/e 21 was small, but that at m/e 20 accounted for about 80% of the total signal measured in the presence of both reagents. The background from CH_3OD alone was found also when CH_3OD was injected directly into the mass spectrometer vacuum chamber and was ascribed to D_2O impurity in the CH_3OD. The mode of correction for the background from F atoms alone (see Results section) is valid only if this background is generated completely *before* or *in* the F_2 discharge. This was tested by studying the reaction of F with CD_3OD. Background signals were comparable to those from F + CH_3OD; however, the standard analysis of the m/e 20 and 21 signals gave [HF]/[DF] = 0.02 ± 0.07, lending confidence to this method of analysis.

The present results show that the less exothermic channel, which yields CH_3O, is the major path for the F + CH_3OH reaction. The data do not provide evidence of a significant isotope effect for the branching fraction. Previous data reveal great uncertainty as regards both the branching fraction and the size of the isotope effect. Several groups[9-11] have compared the total intensities of HF and DF IR chemiluminescence from reaction of F atoms with CH_3OD or CD_3OH. After inclusion of estimated data for v = 0, branching fractions for methoxy formation of 0.50 (CH_3O),[9] 0.31 ± 0.03 (CH_3O),[10] 0.38 ± 0.24 (CH_3O),[11] and 0.63 ± 0.15 (CD_3O)[11] were obtained. Meier et al.[7] have compared the yield of CH_2OH from the reactions of Cl and F with CH_3OH and derived a branching fraction for CH_3O formation of 0.59 ± 0.06. More recently, Bogan and co-workers[12] have reported branching fractions by two independent techniques, involving LEF detection of CH_3O and visible vibration–rotation chemiluminescence from HF and DF; their values range from 0.35 to 0.73.

Although uncertainty remains concerning the exact branching fractions, all studies agree that, despite the lower exothermicity of abstraction of the hydroxyl H atom, this channel accounts for considerably more than the statistical fraction of one-quarter of this reaction.

Comparison of the Product Yields. The CH_3O yields of the reactions of methanol with OH (~0.15) and F (~0.75) can be simply rationalized. The very exothermic F + CH_3OH reaction occurs with a negligible activation energy. The CH_3O yield of this reaction therefore reflects the A factors of the two product channels ($A_{2a} = 1.5 \times 10^{-10}$ cm^3 s^{-1} and $A_{2b} = 5.0 \times 10^{-11}$ cm^3 s^{-1}). The "steric" preference for attack on the hydroxyl hydrogen appears to persist in the OH + CH_3OH reaction where it is manifested in the channel-specific A factors ($A_{1a} = (2.4^{+4.3}_{-1.1}) \times 10^{-11}$ cm^3 s^{-1} and $A_{1b} = (6.2 \pm 2.4) \times 10^{-12}$ cm^3 s^{-1}) obtained from the temperature dependence[6] of the CH_3O yield. In the OH + CH_3OH reaction, however, the activation energies are not negligible, with the larger barrier in the CH_3O channel skewing the product distribution in favor of the CH_2OH channel at room temperature. The fact that the A factors are larger for the F atom reaction than for the OH reaction may be due to the rotational degrees of freedom lost by OH in forming a tight transition state.

Acknowledgment. We acknowledge support of this work by AFOSR Grant 85-0166 and thank Dr. Joe Durant and Mr. Alfred Moyle for helpful discussions.

Registry No. CH_3OH, 67-56-1; OH, 3352-57-6; F, 14762-94-8; CH_3O, 2143-68-2; CH_2OH, 2597-43-5; HF, 7664-39-3; D_2, 7782-39-0.

Rate Constants for H + O_2 + M from 298 to 639 K for M = He, N_2, and H_2O

K.-J. Hsu,[†] S. M. Anderson,[‡] J. L. Durant,*[§] and F. Kaufman[⊥]

Department of Chemistry, University of Pittsburgh, Pittsburgh, Pennsylvania 15260 *(Received: May 28, 1987; In Final Form: September 9, 1987)*

The reaction H + O_2 + M → HO_2 + M (M = He, N_2, and H_2O) has been studied from 298 to 639 K in the third-order regime by use of a high-pressure discharge flow apparatus. Relative rate constants, k_M/k_{He}, derived from these measurements show definite temperature dependences, highlighting the change in relative bath gas efficiencies with temperature. The rate data are well-represented in Arrhenius form, with $k(He) = (4.0 \pm 1.2) \times 10^{-33} \exp[(560 \pm 100)/T]$, $k(N_2) = (6.5 \pm 2.2) \times 10^{-33} \exp[(680 \pm 110)/T]$, and $k(H_2O) = (1.9 \pm 0.9) \times 10^{-32} \exp[(1050 \pm 140)/T]$. Use of total collision rates as the reference collision rate is seen to account for the large M effect observed for H_2O as a third body.

Introduction

The termolecular recombination reaction

$$H + O_2 + M \rightarrow HO_2 + M \quad (1)$$

is of importance in atmospheric as well as flame environments. In the atmosphere it is responsible for the efficient conversion of free H to HO_2;[1] at intermediate temperatures its rate, relative to the bimolecular channel

$$H + O_2 \rightarrow OH + O \quad (2)$$

essentially fixes the second explosion limit in the H_2/O_2 system.[2] At still higher temperatures it has been shown to be important in the postflame region of fuel lean flames.[3] The efficiencies of various bath gases in promoting recombination varies widely, with H_2O being about 25 times more efficient than He at room temperature. Thus, the importance of adequately characterizing reaction 1 over a broad temperature range with a variety of third bodies becomes apparent.

[†] Present address: Mail Stop 183-301, JPL, Pasadena, CA 93111.
[‡] Present address: Aerodyne Research Inc., 45 Manning Road, Billerica, MA 01821.
[§] Present address: Combustion Research Facility, Sandia National Laboratories, Livermore, CA 94550.
[⊥] Deceased July 6, 1985.

(1) Brasseur, B.; Solomon, S. *Aeronomy of the Middle Atmosphere: Chemistry and Physics of the Stratosphere and Mesosphere*; D. Reidel: Boston, 1984.
(2) Dixon-Lewis, G.; Williams, D. J. In *Comprehensive Chemical Kinetics*: Bamford, C. H.; Tipper, C. F. H. Eds.; Elsevier: Amsterdam, 1977; Vol. 17.
(3) Dixon-Lewis, G.; Greenberg, J. B.; Goldsworthy, F. A. *Symp. (Int.) Combust., [Proc.], 15th* **1974**, 717. (b) Westbrook, C. K.; Dryer, F. L. *Prog. Energy Combust. Sci.* **1984**, *10*, 1.

0022-3654/89/2093-1018$01.50/0

Previous studies of the temperature dependence of the recombination have concentrated on temperatures between 200 and 400 K[4-6] or in excess of 950 K.[3,7-14] Additionally, there are a few studies of the H_2/O_2 second explosion limit near 800 K.[15,16] Studies at high temperatures are, in general, complicated by secondary reactions, the most troublesome of which is reaction 2.

A variety of flame studies have attempted to evaluate a rate for (1).[3,8,9] They have relied on models incorporating known and estimated rate constants to simulate experimentally measured flame properties. However, the lack of knowledge concerning the form of the temperature dependence for reaction 1 and the relative efficiencies of various bath gases, together with the lack of uniqueness present in the rate coefficients derived from the model, hamper this effort.

The lack of a single coherent set of data covering a sufficiently broad temperature range has hindered representation of the temperature dependence of (1). With reliable rates existing only at room temperature and around 1000 K, equally good fits can be made to $k = AT^n$, $k = A\exp(-E/kT)$, or $k = AT^n\exp(-E/kT)$, each of which has a vastly different behavior when extrapolated to stratospheric or postflame conditions. To remedy this situation, we have used our newly constructed, high-temperature/high-pressure discharge flow apparatus to study reaction 1 from room temperature to 639 K for the bath gases He, N_2, and H_2O.

Experimental Section

The discharge flow apparatus used in this work has been described in detail earlier.[17,18] It is essentially of standard design, with a stationary H atom source and movable injector for O_2 addition. The major deviation from conventional configurations is the inclusion of a sampling orifice between the flow tube and the detection cell. This allows the flow tube to be operated at pressures up to 70 Torr, while the detection cell pressure can be maintained at about 1 Torr. This pressure drop essentially stops all reaction; we therefore do not need to heat the detection cell. The detection cell is equipped for resonance fluorescence detection of H, OH and, by chemical titration, HO_2.

For the present work we have added a 95-cm-long furnace which allows us to heat the flow tube and sampling orifice to ~1000 K. The furnace was constructed by first placing a copper sleeve around the quartz flow tube. This served to reduce axial temperature gradients. Heat was provided by a three-piece electric heating mantle. Glass wool insulation was used, and the entire furnace was enclosed in a Transite box. Temperatures were measured with four thermocouples mounted on the outside of the flow tube. These measured temperatures agreed with direct measurements made by a thermocouple mounted on a movable probe in the flow tube. Temperature fluctuations within the reaction zone were less than ±2 K over the course of a day, with the axial temperature being uniform to within ±3 K.

For work at temperatures less than 400 K the flow tube and injector were coated with halocarbon wax to reduce radical wall loss rates. At temperatures above 400 K, however, the mobility of the wax was high enough that it began to coat the windows in the unheated detection cell. As a result, we were forced to use bare quartz for $T > 400$ K. It was found that careful washing in 5% HF followed by rinsing with deionized water still gave acceptably low wall loss rates ($k_w(H) < 3\ s^{-1}$, $k_w(OH) < 20\ s^{-1}$).

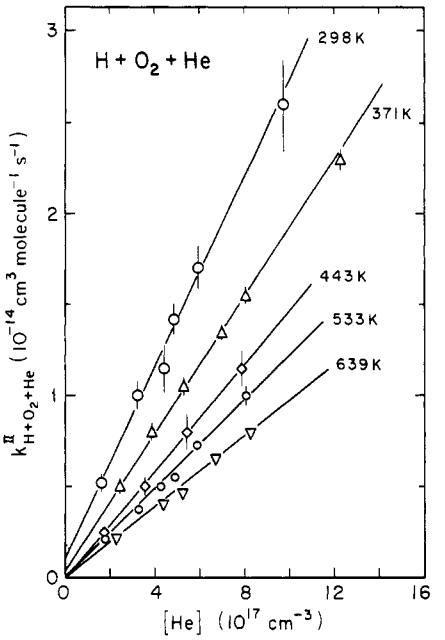

Figure 1. Third-order plot for M = He.

TABLE I: Third-Order Rate Constants (k, 10^{-32} cm^6·s^{-1}) and Total Collision Rates (Z, 10^{-9} cm^3 s^{-1})

	M = He		M = N_2		M = H_2O	
T, K	k	Z	k	Z	k	Z
298	2.6 ± 0.3	2.0	6.0 ± 0.8	3.0	64 ± 12	51
371	1.8 ± 0.2	2.1	4.6 ● 0.7	3.2	36 ± 8	51
433	1.5 ± 0.2	2.3	3.4 ± 0.5	3.3	21 ± 5	51
533	1.2 ± 0.3	2.4	2.3 ± 0.6	3.5	13 ± 5	51
639	0.91 ± 0.15	2.5	1.7 ± 0.3	3.8	10 ± 2	51

For most of the data presented here, H atoms were produced by means of a resistively heated dissociator.[17,19] This provided an O and OH free radical source but required $[H_2] \cong 2 \times 10^{14}$ cm^{-3} due to its low efficiency (about 1%) for atom production. At room temperature under our typical operating conditions ($[H]_0 \approx 2 \times 10^{12}$, $[O_2] \approx 1 \times 10^{16}$, $P = 5$–70 Torr) this is not a problem, but at higher temperatures the reaction OH + H_2 → H + H_2O becomes increasingly important, recycling H through the partial mechanism

$$H + O_2 + M \rightarrow HO_2 + M \quad (1)$$

$$HO_2 + H \rightarrow 2OH \quad (3a)$$

$$OH + H_2 \rightarrow H + H_2O \quad (4)$$

To overcome this problem, we used a microwave discharge to produce H atoms for those studies. This allowed $[H_2]$ to be reduced by a factor of 100, permitting kinetic measurements to higher temperatures. To reduce O and OH from the microwave discharge to acceptable levels, we further purified the UHP He by passage through a copper wool packed oven which was heated to 700 K, followed by two molecular sieve traps held at 77 K. Our high-temperature limit of 650 K is dictated by the increasing predominance of

$$H + O_2 \rightarrow OH + O \quad (2)$$

which becomes the primary reaction channel at high temperature

(4) Clyne, M. A.; Thrush, B. *Proc. R. Soc. London* **1963**, *A275*, 559.
(5) Kurylo, M. J. *J. Phys. Chem.* **1972**, *76*, 3518.
(6) Wong, W.; Davis, D. D. *Int. J. Chem. Kinet.* **1974**, *6*, 401.
(7) Skinner, G. B.; Ringrose, G. H. *J. Chem. Phys.* **1965**, *42*, 2190.
(8) Fenimore, C. P.; Jones, G. W. *Symp. (Int.) Combust., [Proc.], 10th* **1965**, 717.
(9) Dixon-Lewis, G.; Williams, A. *Symp. (Int.) Combust., [Proc.], 11th* **1967**, 951.
(10) Getzinger, R. W.; Schott, G. L. *J. Chem. Phys.* **1965**, *43*, 3237.
(11) Getzinger, R. W.; Blair, L. S. *Combust. Flame* **1969**, *13*, 271.
(12) Blair, L. S.; Getzinger, R. W. *Combust. Flame* **1970**, *14*, 5.
(13) Gutman, D.; Hardwidge, E. A.; Dougherty, F. A.; Lutz, R. W. *J. Chem. Phys.* **1967**, *47*, 4400.
(14) Slack, M. W. *Combust. Flame* **1977**, *28*, 241.
(15) Dixon-Lewis, G.; Linnett, J. W. *Trans. Faraday Soc.* **1953**, *49*, 756.
(16) Baldwin, R. R.; Jackson, D.; Walker, R. W.; Webster, S. J. *Trans. Faraday Soc.* **1967**, *63*, 1676.
(17) Hsu, K.-J.; Durant, J. L.; Kaufman, F. *J. Phys. Chem.* **1987**, *91*, 1895.
(18) Hsu, K.-J. Ph.D. Thesis, University of Pittsburgh, 1986.
(19) Trainor, D. W.; Ham, D. O.; Kaufman, F. *J. Chem. Phys.* **1973**, *58*, 4599.

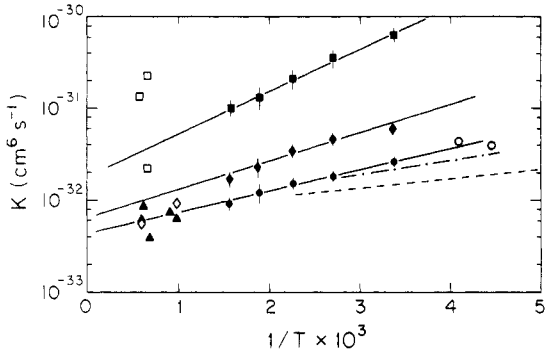

Figure 2. Arrhenius plot of H + O_2 + M third-order rate constants: squares, M = H_2O; diamonds, M = N_2; circles, M = He; triangles, M = Ar. Points with error bars are from this study. Dashed line is from ref 5 for He and Ar; dashed-dotted line is from ref 6 for He and Ar. Other data are from ref 4 and 8–14.

for our range of accessible pressures.

Data analysis followed the protocol discussed extensively in our room-temperature study.[17] The list of secondary reactions included in our computer model was expanded to include the reaction of H with O_2 and O with H_2. Figure 1 shows typical data obtained for M = He.

Results and Discussion

Our temperature-dependent rate constants for H + O_2 + M (M = He, N_2, and H_2O) are listed in Table I and plotted, together with results of other studies for M = He, Ar, N_2, and H_2O, in an Arrhenius plot in Figure 2. Our data can be represented by a $k = AT^n$ relationship, with

$$k(\mathrm{He}) = (3.2 \pm 0.5) \times 10^{-32}(T/300)^{-(1.3\pm0.2)}$$

$$k(\mathrm{N_2}) = (6.2 \pm 1.2) \times 10^{-32}(T/300)^{-(1.66\pm0.25)}$$

$$k(\mathrm{H_2O}) = (6 \pm 4) \times 10^{-30}(T/300)^{-(2.5\pm0.2)}$$

where the quoted uncertainties are ±1 σ.

There have been only three previous studies of the temperature dependence of (1) in the region around room temperature. Clyne and Thrush[4] used the discharge flow technique to study the reaction for M = He from 225 K to room temperature. The analysis of their data relied on knowing the branching fraction for reaction 3

$$\mathrm{H + HO_2 \rightarrow 2OH} \quad (3a)$$

$$\rightarrow \mathrm{H_2O + O} \quad (3b)$$

$$\rightarrow \mathrm{H_2 + O_2} \quad (3c)$$

which they were forced to measure indirectly. The branching fraction has since been directly measured[20] and its temperature independence established.[21] As in our room-temperature study,[17] we have corrected Clyne and Thrush's reported rate, using the directly measured branching fraction. Two other studies[5,6] utilized flash photolysis; however, their rates at room temperature are at variance with the bulk of the other room-temperature studies,[17] and their temperature dependences are at variance with one another.

If we include the corrected low-temperature data of Clyne and Thrush[4,17] on a log k vs log T plot, we note the presence of curvature in the M = He data. This curvature is not present in the Arrhenius plot, Figure 2, and thus we favor an Arrhenius representation of our data, with

$$k(\mathrm{He}) = (4.0 \pm 1.2) \times 10^{-33} \exp[(560 \pm 100)/T]$$

$$k(\mathrm{N_2}) = (6.5 \pm 2.2) \times 10^{-33} \exp[(680 \pm 110)/T]$$

$$k(\mathrm{H_2O}) = (1.9 \pm 0.9) \times 10^{-32} \exp[(1050 \pm 140)/T]$$

Our rate expression for M = He is in agreement with Baulch et al.,[22] who recommend

$$k(\mathrm{He}) = 4.1 \times 10^{-33} \exp(500/T) \pm 50\%, \quad 300 \le T \le 2000 \text{ K}$$

Our data, expressed as $k = AT^n$, also agrees, within error bars, with the newer NASA/JPL evaluation.[23]

Shock tube studies of induction times in H_2/O_2/bath gas systems are the least complex methods to evaluate k_1 in the vicinity of 1000 K. The identity of the bath gas is known, and the principal chemistry is well-described by reactions

$$\mathrm{H_2 + O_2 \rightarrow O, H, OH} \quad (5)$$

$$\mathrm{H + O_2 \rightarrow OH + O} \quad (2)$$

$$\mathrm{O + H_2 \rightarrow OH + H} \quad (6)$$

$$\mathrm{OH + H_2 \rightarrow H_2O + H} \quad (4)$$

$$\mathrm{H + O_2 + M \rightarrow HO_2 + M} \quad (1)$$

An early study of this type was carried out by Gutman and co-workers.[13] Their induction time measurements were modeled by a five-reaction sequence, which could be solved to yield the induction time as the real root of a third-order polynomial. The solution is found to be independent of k_5, with the coefficients made up of sums and products of rate constants for reactions 1, 2, 4, and 6. The original analysis used a value for k_4 which was about a factor of 10 below the presently accepted value.[23] This was then combined with low- and high-density shock data to extract the other three rate constants. The degree of agreement between Gutman et al.'s values for k_2 and k_6 and presently accepted values supports their conclusion that the rate constants were fairly insensitive to the input value of k_4. We have reevaluated their published data using presently accepted values for the three known rate constants. The resulting rate, $k_1(\mathrm{Ar}) = (7.4 \pm 2.2) \times 10^{-33}$ cm^6 s^{-1} for T = 1100–1600 K, is only about 20% lower than Gutman et al.'s original evaluation.

Slack[14] has evaluated $k_1(\mathrm{N_2})$ in the range from 980 to 1176 K based on his own measurements and reevaluated the data of Skinner and Ringrose[7] for k_1(Ar) between 964 and 1075 K. This latter rate is in good agreement with our reevaluation of Gutman et al.'s shock tube data. Over the ~600 K temperature interval studied (950–1550 K), no temperature dependence can be discerned above the uncertainties in the individual rate constant measurements.

Getzinger and co-workers[10-12] have attempted to directly measure k_1 at temperatures of 1400–1870 K by studying the long time relaxation of shock heated H_2/O_2/M mixtures. They divided the time evolution of their shock-heated mixtures into two regimes. Shortly after passage of the shock front partial equilibration is achieved, with [O], [OH], and [H] being in a steady state, defined by the fast bimolecular reactions in the shock-heated gas. Thereafter, the mixture relaxed toward full equilibrium, with H + O_2 + M assumed to be the controlling reaction. The large scatter in their reported rate constants attests to the difficulties inherent in extracting reliable rate constants from such measurements.

The discrepancies in literature values for $k_1(\mathrm{H_2O})$ at $T > 1000$ K make the temperature dependence of the relative third-body efficiencies, k_M/k_{He}, uncertain. Although some data have been analyzed assuming that k_M/k_{He} is temperature independent, our measurements clearly indicate that this is not the case for H + O_2 + M, as can be seen in Figure 3 where we have plotted log (k_M/k_{He}) vs log (T) for M = N_2 and H_2O. Since log–log plots are notoriously linear, we are not surprised by (nor do we ascribe

(20) Sridharan, U. C.; Qiu, L. X.; Kaufman, F. *J. Phys. Chem.* **1982**, *86*, 4569.

(21) Keyser, L. F. *J. Phys. Chem.* **1986**, *90*, 2994.

(22) Baulch, D. L.; Drysdale, D. D.; Horne, D. G.; Lloyd, A. C. *Evaluated Kinetic Data for High Temperature Reactions*; CRC: Cleveland, 1972; Vol. 1.

(23) DeMore, W. B.; et al. "Chemical Kinetics and Photochemical Data for Use in Stratospheric Modeling"; Evaluation No. 6; NASA-JPL: Pasadena, CA, 1983.

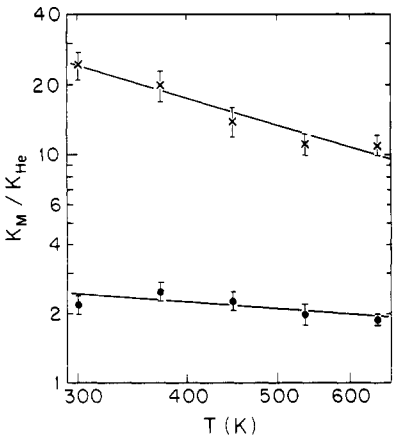

Figure 3. Temperature dependence of relative third-body efficiencies, k_M/k_{He}: circles, M = N_2; crosses, M = H_2O.

importance to) the observed linear behavior. Least-squares fits were performed to quantify the behavior, yielding

$$k_M/k_{He} = 2.47(T/300)^{-0.37}; \quad M = N_2$$

$$k_M/k_{He} = 23.9(T/300)^{-1.18}; \quad M = H_2O$$

for 298 < T < 635 K.

The behavior of N_2 relative to He we observe correctly predicts the relative rates for N_2 and Ar seen by Slack,[14] $k(N_2)/k(Ar)$ = 1.5 at $T \sim 1050$ K. Moreover, extrapolation of our data for M = He to high-temperature passes through the Ar data of Slack[14] and Gutman.[13] We thus see evidence that the similarity in rate constants observed for He and Ar at room temperature continues to higher temperatures.

It has become customary to use the formalism introduced by Troe[24] to interpret recombination rate data. In the low-pressure, third-order regime we can write,[17] following Troe[24]

$$k = \beta_c Z_{LJ} k^{sc}_{AB}$$

where β_c is the collision efficiency, Z_{LJ} is the Lennard-Jones collision rate,[24] and k^{sc}_{AB} is made up of a collection of factors which can be calculated from properties of the two recombining species.

We have previously noted that use of the Lennard-Jones collision rate

$$Z_{LJ} = \pi\sigma^2(8kT/\pi\mu)^{1/2}\Omega^{*(2,2)}$$

leads to β_c values greater than 1.[17] Thus, following our earlier approach,[17] we choose instead to use total collision rates[25] (referred to as total scattering rates in ref 17) as reference collision rates. Semiclassically, the total collision rate assigns equal weight to all trajectories which are deflected through an angle larger than the Heisenberg uncertainty limiting angle. It thus represents an upper limit for any collision process. Calculation of the total collision rate requires knowledge of the Lennard-Jones radius, σ, and well depth, ϵ, as well as the dipole moments of the molecules. For bath gases with negligible dipole moments the total collision rates were calculated from a thermal average of the Schiff–Landau–Lifshitz formula[25]

$$Z = 7.64 \times 10^{-12}(\epsilon\sigma^6)^{0.4}(T/\mu)^{0.3}$$

(24) Troe, J. *J. Phys. Chem.* **1979**, *83*, 114.

TABLE II: Molecular Parameters Used

	HO_2	He	N_2	H_2O
σ, Å	3.43[a]	2.576[c]	3.68[c]	2.71[d]
ϵ/k, K	289[a]	10.2[c]	91.5[c]	506[d]
μ, D	2.09[b]	0	0	1.85[e]

[a] Patrick, R.; Golden, D. M. *Int. J. Chem. Kinet.* **1983**, *15*, 1189. [b] Saito, S.; Matsummra, C. *J. Mol. Spectrosc.* **1980**, *80*, 34. [c] Hirschdfelder, J. D.; Curtiss, C. F.; Bird, R. B. *Molecular Theory of Gases and Liquids*; Wiley: New York, 1954; pp 1110–1112. [d] Monchick, L.; Mason, E. A. *J. Chem. Phys.* **1961**, *35*, 1676. [e] Radzig, A. A.; Smirov, B. M. *Reference Data on Atoms, Molecules, and Ions*; Springer-Verlag: New York, 1985; p 442.

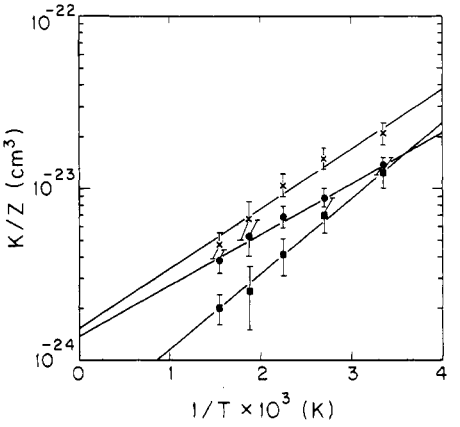

Figure 4. Reduced Arrhenius plot, k/Z vs $1/T$: squares, M = H_2O; crosses, M = N_2; circles, M = He.

For HO_2–H_2O we calculated total collision rates directly, using JWKB and Born formula for phase shifts and treating the dipoles as fixed in orientation during the collision.[25] The calculated total collision rates are listed in Table I. The parameters used in their calculation are listed in Table II.

The key result of this analysis is that the bulk of the variations in third-body efficiencies are accounted for by the differences in the total collision rates. Thus, the factor of 24 difference between $k_{298}(H_2O)$ and k_{298}(He) is balanced by a factor of 25 difference between their respective total collision rates. Figure 4 presents our data reduced by the appropriate total collision rates. We see that the largest spread in reduced rates is just over a factor of 2, between M = N_2 and M = H_2O at 639 K, as contrasted to a spread of a factor of 24 in the unreduced rates. Use of the total collision rate as a reference collision rate is thus seen to correctly account for the majority of the differences in third-body efficiencies observed for various bath gases. Because of this, its use is recommended in the analysis of recombination rate data and in attempts to extrapolate the data to higher to lower temperatures.

Acknowledgment. We acknowledge the help of Dr. P. E. Siska, who made available programs to calculate Born and JWKB phase shifts. We also thank Dr. M. F. Golde. This work was supported by the ARO under Grant DAAG2985K0041.

Registry No. H, 12385-13-6; O_2, 7782-44-7; He, 7440-59-7; N_2, 7727-37-9; H_2O, 7732-18-5.

(25) Durant, J. L.; Kaufman, F. *Chem. Phys. Lett.* **1987**, *142*, 246.